New windows on massive stars: asteroseismology, interferometry, and spectropolarimetry
Proceedings IAU Symposium No. 307, 2014
G. Meynet, C. Georgy, J. H. Groh & Ph. Stee, eds.

doi:10.1017/S1743921314007327

Accretion Signatures on Massive Young Stellar Objects

F. Navarete[1], A. Damineli[1], C. L. Barbosa[2] and R. D. Blum[3]

[1]IAG-USP, Rua do Matão, 1226, 05508-900, São Paulo, SP Brazil
email: navarete@usp.br

[2]UNIVAP, São José dos Campos, SP, Brazil
[3]NOAO, 950 N Cherry Ave., Tuczon, AZ 85719 USA

Abstract. We present preliminary results from a survey of molecular H_2 (2.12 μm) emission in massive young stellar objects (MYSO) candidates selected from the Red *MSX* Source survey. We observed 354 MYSO candidates through the H_2 S(1) 1-0 transition (2.12 μm) and an adjacent continuum narrow-band filters using the Spartan/SOAR and WIRCam/CFHT cameras. The continuum-subtracted H_2 maps were analyzed and extended H_2 emission was found in 50% of the sample (178 sources), and 38% of them (66) have polar morphology, suggesting collimated outflows. The polar-like structures are more likely to be driven on radio-quiet sources, indicating that these structures occur during the pre-ultra compact H II phase. We analyzed the continuum images and found that 54% (191) of the sample displayed extended continuum emission and only ∼23% (80) were associated to stellar clusters. The extended continuum emission is correlated to the H_2 emission and those sources within stellar clusters does display diffuse H_2 emission, which may be due to fluorescent H_2 emission. These results support the accretion scenario for massive star formation, since the merging of low-mass stars would not produce jet-like structures. Also, the correlation between jet-like structures and radio-quiet sources indicates that higher inflow rates are required to form massive stars in a typical timescale less than 10^5 years.

Keywords. Stars: formation, Stars: early-type, Stars: pre-main sequence, ISM: jets and outflows.

1. Introduction

The formation of massive stars ($M > 8\,M_\odot$) is one of the most important problems in stellar astrophysics and is still poorly understood. Two scenarios currently dominate the discussions, assuming that high mass stars are *a*) formed by accretion through a disk (Krumholz *et al.* 2005); or *b*) via coalescence of low mass stars (Bonnell *et al.* 2001). Low and intermediate mass stars are formed by the gravitational collapse of the parental giant molecular cloud (GMC), followed by the accretion process (Palla 1996). However, when a young stellar object (YSO) reaches $8\,M_\odot$, the radiative flux is intenser than in the previous case and may interrupt the accretion flow. A process that collimates the radiation field is required to overcome this effect, such as the bipolar outflows observed in massive YSOs (MYSO). In the second scenario, massive stars are formed by coalescence of low-mass stars in dense clusters (Bonnell *et al.* 2001). Low-mass stars are formed under the accretion scenario, interact with each other, and collide to form stars of larger masses (Stahler *et al.* 2000; Bally *et al.* 2002).

While there is no evidence for stellar mergers in clusters, a growing number of both observational evidences (Bik & Thi 2004; Blum *et al.* 2004) and simulations (Krumholz *et al.* 2009) support the accretion scenario. Recently, MYSO candidates were observed in the H_2 narrow filter and collimated jets were identified, suggesting accretion discs around these objects (Varricatt *et al.* 2010). Although this work presents observational

evidences for the accretion scenario, only a few MYSOs were confirmed on this sample. Although the scenario of an accretion disk may apply for all massive stars, the details are lacking. Instead of doing detailed study of a small number of potential candidates that might harbor a disk, we are moving toward a large statistical study which will point to accretion signatures (or not) of a well selected sample of 354 MYSO candidates, selected by the Red *MSX* Source (RMS) survey (Lumsden *et al.* 2002; Mottram *et al.* 2011, and references therein).

2. Observations and Data Reduction

Our sample of 354 MYSO candidates comprises 135 sources located in the Northern hemisphere ($\delta > 0°$) and 219 from the Southern one ($\delta < 0°$). Most of the Northern sources were observed using the WIRCam camera deployed at the Canada-France-Hawaii Telescope (CFHT, Hawaii) while the Southern objects were observed using the Spartan and OSIRIS cameras at the Southern Astrophysical Research Telescope (SOAR, Chile). Each source was observed through the H_2 ($\lambda \approx 2.12\,\mu$m, $\Delta\lambda \approx 0.03\,\mu$m) and K-band continuum ($\lambda \approx 2.2\,\mu$m, $\Delta\lambda \approx 0.03\,\mu$m) narrow-band filters, using a total exposure time of ~ 600 seconds per filter. The data was processed using THELI, an instrument-independent pipeline for automated reduction of astronomical images (Erben *et al.* 2005; Schirmer 2013). Each H_2 processed image was continuum-subtracted, scaling its narrow-band K-band continuum image. This procedure was adopted in order to subtract the continuum emission at the same wavelength range and the usage of narrow filters avoided the contamination of the H_2 emission by nebular features such as Brackett-γ.

3. Results

The continuum-subtracted H_2 maps were analyzed and each source was classified according to the following properties:

a) Classification of Extended H_2 emission: four classes were defined to classify the H_2 emission (each type is illustrated in Figure 1): 1) Polar emission (BPn): those extended H_2 emission are likely to be jet-like structures (the "n" corresponds to the number of polar structures: BP1 is monopolar, BP2 is bipolar and BP5 is multipolar emission); 2) Nodal emission (K): K-type morphology corresponds to those sources that display non-aligned knots of H_2 emission; 3) Diffuse emission (D): D-type sources are associated to diffuse H_2 emission, possibly originated by fluorescent excitation of the H_2 molecules; 4) No emission (N): corresponds to the non-detections.

b) NIR Classification of the environment: The environment surrounding each RMS source was classified according to the following properties: *i*) presence of extended continuum emission; and *ii*) association with a stellar cluster.

3.1. *Global analysis of the sample*

The general statistics of the sample is shown in Figure 2. We found extended H_2 emission towards $\approx 50\%$ of the targets (148 sources) while $\sim 54\%$ are associated to extended continuum emission (191). Only $\approx 23\%$ of the sample (80) are apparent members of stellar clusters. The relatively low fraction of sources associated to stellar clusters is an evidence that confronts the merging scenario proposed by Bonnell *et al.* (1998), which cannot explain the formation of roughly $\sim 77\%$ of the observed sources. This result indicates that massive stars require a mechanism that allow their formation even isolated from other stars. Figure 2b displays the morphological classification of the extended H_2 emission as defined on subsection 3. It shows that $\approx 50\%$ of the sample were classified

https://doi.org/10.1017/S1743921314007327 Published online by Cambridge University Press

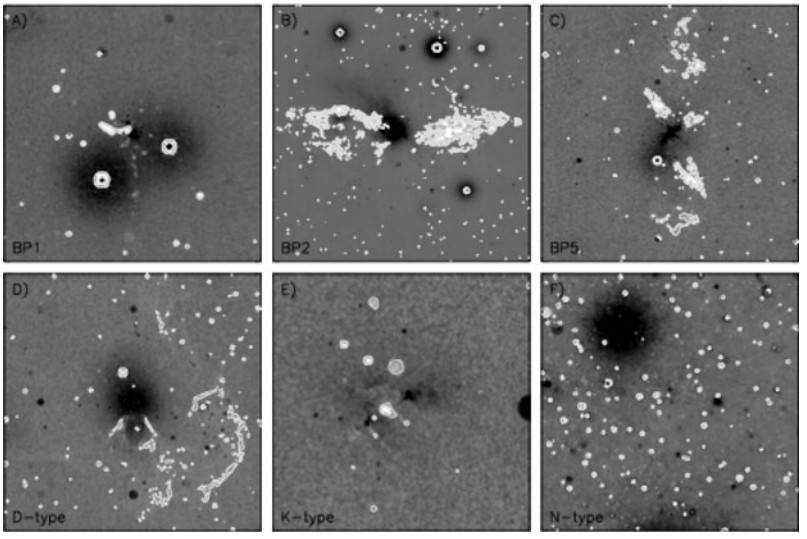

Figure 1. Examples of the morphological classes based on the H_2 emission. The contours are placed at $\sigma = 1.0$ and 3.0. *(a), (b),* and *(c):* BP1-, BP2-, and BP5-type sources, respectively. *(d), (e),* and *(f):* D-, K-, and N-type sources, respectively.

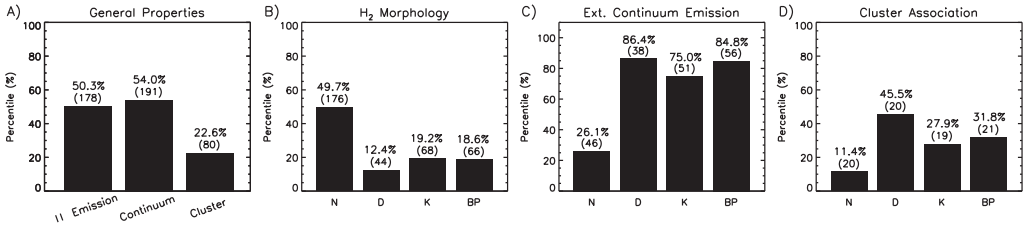

Figure 2. Global properties of the sample. *(a):* detection of extended H_2 and continuum emission and association with stellar clusters; *(b):* morphology of the H_2 emission. *(c):* detection of extended continuum emission as a function of the H_2 morphology. *(d):* association with stellar clusters as a function of the H_2 morphology. The numbers shown at the top of each bar corresponds to the percentage of the sample.

as N-type objects (176 sources), about $\approx 12\%$ displays diffuse H_2 emission (44), $\approx 19\%$ were classified as K-type sources (68) and $\approx 19\%$ sources (66) are associated with polar structures (monopolar, bipolar or multipolar) and were classified as BP-type. Figure 2c displays a correlation between the sources associated to extended H_2 emission (BP-, K- and D-type) with those which display extended continuum emission (roughly $\sim 80\%$ compared to $\sim 25\%$ found for N-type sources). The positive detection of extended continuum emission could be due to two processes: *i*) nebular emission or *ii*) dust-scattered radiation. Our strategy does not allow us to resolve the nature of the continuum emission. Additional observations in atomic transition lines (such as Brackett-γ at 2.16 μm) could trace the gaseous emission associated to such regions. Figure 2d indicates that most stellar clusters with MYSOs also exhibit extended H_2 emission.

3.2. *Radio quiet/loud phases and H_2 morphology*

The RMS sources were classified as radio quiet (YSO) or radio loud (HII) sources based on 6 cm observations made by Urquhart *et al.* (2007, 2009). Our sample consists of 282 radio quiet sources and 72 radio loud ones. Figure 3 displays the global results of the survey but separated between radio quiet/loud sources. Panel (a) shows the fraction of

https://doi.org/10.1017/S1743921314007327 Published online by Cambridge University Press

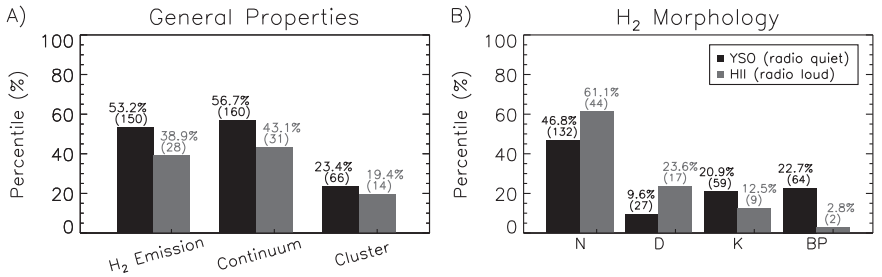

Figure 3. Same as *(a)* and *(b)* of Fig. 2, but separated between radio quiet (YSO, in black) and radio loud (HII, in grey) sources.

radio quiet sources associated to both extended H_2 and continuum emission is $\sim 10\%$ larger than the values found for radio loud ones. The fraction of radio quiet or radio loud sources associated to stellar clusters is almost the same ($\sim 20\%$). Panel (b) indicates the fraction of radio loud sources increases in the opposite direction of the radio quiet ones: YSOs are more often associated to BP-type emission while D-type emission is found towards HII regions.

3.3. *Polar structures and comparison with other samples*

Varricatt *et al.* (2010) present a similar survey based on a smaller sample of 50 MYSO candidates. They found extended H_2 emission towards 38 of them (76%) and 25 sources were associated to polar H_2 structures, suggesting collimated jets. The fraction of the sources associated with extended H_2 emission and those that present polar structures are 1.5 and 2.7 times the values found on the present work (50.3 and 18.6%, respectively).

Figure 4 displays the distribution of the projected length ($\ell_{\rm proj}$) and the aspect ratio (R) of the polar structures as a function of the bolometric luminosity of the RMS source. Panel (a) shows a slight tendency that $\ell_{\rm proj} \propto (L/L_{\odot})$ on di-log scales. The plot also indicates that the data from Varricatt *et al.* (2010) display $\ell_{\rm proj} \lesssim 2\,$pc, while those from our sample are up to ~ 10 times bigger. The overall conclusion from the plot is that high-luminosity sources can drive massive and powerful structures that extends up to $\sim 10\,$pc while low-luminosity ones cannot produce very extended structures. This result also indicates the size of the jets are related to intrinsic characteristics of their driven source.

Figure 4b indicates that high-collimated ($R \gtrsim 10$) structures are found on the entire range of luminosities on the present work while the sample from Varricatt *et al.* (2010) displays only three high-collimated structures associated to sources with $3 \lesssim \log(L/L_{\odot}) \lesssim 5$. Our sample presents several polar structures driven by high-luminosity sources ($\log(L/L_{\odot}) \gtrsim 4.0$) that are less collimated ($R \lesssim 2.0$) than those found by Varricatt *et al.* (2010). On the other hand, there is no correlation between R values as a function of the luminosity of the central source, indicating that outflows driven by MYSOs have a similar collimation mechanism than those found toward YSOs.

4. Summary and Conclusions

We observed a sample of 354 MYSOs in the H_2 narrow-filter at $2.12\,\mu$m and an adjacent continuum narrow-band filter. The analysis of each H_2-map revealed that:

(*a*) 50% of our sources display extended H_2 emission: 19% exhibit polar structures, 19% are associated to nodal or amorphous emission and $\approx 12\%$ corresponds to diffuse H_2 emission;

https://doi.org/10.1017/S1743921314007327 Published online by Cambridge University Press

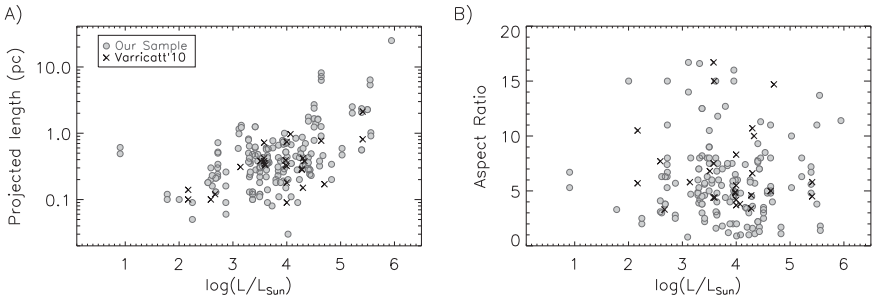

Figure 4. Distribution of the projected length of the structures classified as BP-type *a* and their aspect ratio (*b*) as a function of the logarithm of the luminosity of the driven RMS source. Data from this work is shown as filled grey circles while those from Varricatt *et al.* (2010) are shown as × symbols.

(*b*) We found a considerable number of objects (66) associated to collimated structures and bipolar outflows and most of them are radio quiet sources. This is an observational evidence for the accretion scenario and suggests that MYSOs are formed through discs and most of the accretion occurs on timescales less than 10^5 years;

(*c*) We found a tendency that larger structures are found towards high-luminosity sources. The low-luminosity counterpart cannot drive very extended jets or even be associated to diffuse emission, which requires higher radiative fluxes;

(*d*) We could not establish a correlation between the collimation factor of the polar structures and the bolometric luminosity of their driven sources;

(*e*) The number of sources associated to stellar clusters (high density environments) are much less than the expected for the coalescence scenario, indicating that the merging of low mass stars cannot be the main scenario for massive star formation.

References

Bally, J., Reipurth, B., Walawender, J., & Armond, T. 2002, *AJ* 124, 2152
Bik, A. & Thi, W. F. 2004, *A&A* 427, L13
Blum, R. D., Barbosa, C. L., Damineli, A., Conti, P. S., & Ridgway, S. 2004, *ApJ* 617, 1167
Bonnell, I. A., Bate, M. R., Clarke, C. J., & Pringle, J. E. 2001, *MNRAS* 323, 785
Bonnell, I. A., Bate, M. R., & Zinnecker, H. 1998, *MNRAS* 298, 93
Erben, T., Schirmer, M., Dietrich, J. P., *et al.* 2005, *Astronomische Nachrichten* 326, 432
Krumholz, M. R., Klein, R. I., McKee, C. F., Offner, S. S. R., & Cunningham, A. J. 2009, *Science* 323, 754
Krumholz, M. R., McKee, C. F., & Klein, R. I. 2005, *ApJ* 618, L33
Lumsden, S. L., Hoare, M. G., Oudmaijer, R. D., & Richards, D. 2002, *MNRAS* 336, 621
Mottram, J. C. *et al.* 2011, *A&A* 525, A149
Palla, F. 1996, in S. Beckwith, J. Staude, A. Quetz, & A. Natta (eds.), *Disks and Outflows Around Young Stars*, Vol. 465 of *Lecture Notes in Physics, Berlin Springer Verlag*, p. 143
Schirmer, M. 2013, *ApJS* 209, 21
Stahler, S. W., Palla, F., & Ho, P. T. P. 2000, *Protostars and Planets IV* p. 327
Urquhart, J. S., Busfield, A. L., Hoare, M. G., *et al.* 2007, *A&A* 461, 11
Urquhart, J. S. *et al.* 2009, *A&A* 501, 539
Varricatt, W. P., Davis, C. J., Ramsay, S., & Todd, S. P. 2010, *MNRAS* 404, 661

Discussion

IBADOV: Have you any manifestations of the fall of large comet-like objects onto young massive stars?

https://doi.org/10.1017/S1743921314007327 Published online by Cambridge University Press

Navarete: Since we are working with large-scale structures (a few parsecs), I don't think it would be possible to observe these comet-like objects in our maps. It would be better to work with higher angular resolution observations in order to resolve the innermost region around the circumstellar medium of MYSOs and –perhaps– observe these kind of phenomena.

Ibadov: Will you study them in the future?

Navarete: We are planning to work with high angular resolution data from NIFS (Gemini north) to study the accretion process "in situ" and then move to longer wavelength (APEX, ALMA) to conclude the work. If there are any evidences of flares or even the comet-like objects associated to the accretion process, these data could reveal them.

Groh: Could you comment on how accurate the luminosity and distance determinations are?

Navarete: The luminosity of the sources are based in the bolometric fluxes derived by Mottram *et al.* (2011) and the kinematic distances derived from ^{13}CO observations by Urquhart *et al.* (2007, 2008). The major source of uncertainty of the bolometric fluxes determination comes from the fittings that do not have far-infrared fluxes. The worst cases could have an error up to 50% of the bolometric flux value. Regarding the distance determination, the ^{13}CO line is more likely to be associated to the source itself than the ^{12}CO one, which could display a complex structure due to the presence of larger structures on the line-of-sight.

Felipe Navarete

https://doi.org/10.1017/S1743921314007327 Published online by Cambridge University Press